

Accepted Manuscript

Systemic effects of Subtilase cytotoxin produced by *Escherichia coli* O113:H21

E. Abril Seyahian, Gisela Oltra, Federico Ochoa, Santiago Melendi, Ricardo Hermes, James C. Paton, Adrienne W. Paton, Nestor Lago, Mauricio Castro Parodi, Alicia Damiano, Cristina Ibarra, Elsa Zotta



PII: S0041-0101(16)30869-8

DOI: [10.1016/j.toxicon.2016.12.014](https://doi.org/10.1016/j.toxicon.2016.12.014)

Reference: TOXCON 5532

To appear in: *Toxicon*

Received Date: 20 October 2016

Revised Date: 28 December 2016

Accepted Date: 31 December 2016

Please cite this article as: Seyahian, E.A., Oltra, G., Ochoa, F., Melendi, S., Hermes, R., Paton, J.C., Paton, A.W., Lago, N., Castro Parodi, M., Damiano, A., Ibarra, C., Zotta, E., Systemic effects of Subtilase cytotoxin produced by *Escherichia coli* O113:H21, *Toxicon* (2017), doi: 10.1016/j.toxicon.2016.12.014.

This is a PDF file of an unedited manuscript that has been accepted for publication. As a service to our customers we are providing this early version of the manuscript. The manuscript will undergo copyediting, typesetting, and review of the resulting proof before it is published in its final form. Please note that during the production process errors may be discovered which could affect the content, and all legal disclaimers that apply to the journal pertain.

1 **Systemic effects of Subtilase cytotoxin produced by *Escherichia coli* O113:H21**

2

3 **E. Abril Seyahian^a, Gisela Oltra^a, Federico Ochoa^a, Santiago Melendi^a, Ricardo Hermes^b,**
4 **James C. Paton^c, Adrienne W. Paton^c, Nestor Lago^d, Mauricio Castro Parodi^a, Alicia**
5 **Damiano^a, Cristina Ibarra^a, Elsa Zotta^{a,e#}**

6

7 ^aUniversidad de Buenos Aires, Facultad de Medicina. Instituto de Fisiología y Biofísica
8 IFIBIO Houssay-CONICET, ^bHospital de Agudos Juan A. Fernandez, Laboratorio Central,
9 ^cUniversity of Adelaide Research, Department of Molecular and Cellular Biology, Centre for
10 Infectious Diseases, Australia. ^dUniversidad de Buenos Aires. Facultad de Medicina.
11 Laboratorio de Patología Experimental y Aplicada, ^eUniversidad de Buenos Aires. Facultad
12 de Farmacia y Bioquímica. Cátedra de Fisiopatología. Buenos Aires, Argentina.

13

14 Running Head: Systemic effects of Subtilase cytotoxin

15

16 #Address correspondence to Elsa Zotta, ezotta@fmed.uba.ar. Paraguay 2155, CABA

17 (1121). Buenos Aires, Argentina. Tel. +54 11 5950 9500 int 2141

18 **ABSTRACT**

19

20 Subtilase cytotoxin (SubAB) is a member of the AB₅ cytotoxin family and is produced by
21 certain strains of Shiga toxigenic *Escherichia coli*. The toxin is known to be lethal to mice,
22 but the pathological mechanisms that contribute to Uremic Hemolytic Syndrome (HUS)
23 are poorly understood. In this study we show that intraperitoneal injection of a sublethal
24 dose of SubAB in rats triggers a systemic response, with ascitic fluid accumulation, heart
25 hypertrophy and damage to the liver, colon and kidney. SubAB treated rats presented
26 microalbuminuria 20 days post inoculation. At this time we found disruption of the
27 glomerular filtration barrier and alteration of the protein reabsorption mechanisms of the
28 proximal tubule. In the kidney, SubAB also triggered an epithelial to mesenchymal
29 transition (1). These findings indicate that apart from direct cytotoxic effects on renal
30 tissues, SubAB causes significant damage to the other organs, with potential
31 consequences for HUS pathogenesis.

32 Importance: Uremic Hemolytic Syndrome is an endemic disease in Argentina, with over
33 400 hundred new cases each year. We have previously described renal effects of Shiga
34 Toxin and its ability to alter renal protein handling. Bearing in mind that Subtilase
35 Cytotoxin is an emerging pathogenic factor, that it is not routinely searched for in patients
36 with HUS, and that to the date its systemic effects have not been fully clarified we decided
37 to study both its systemic effects, and its renal effects to assess whether SubAB could be
38 contributing to pathology seen in children.

39

40 **1. INTRODUCTION**

41

42 Hemolytic Uremic Syndrome (HUS) results from the action of multiple factors. It is defined
43 by a triad of microangiopathic hemolytic anemia, thrombocytopenia and acute kidney
44 failure. It's typical form can be triggered after infection by Shiga-toxigenic *Escherichia coli*
45 (STEC). These bacteria are known to produce Shiga toxin (Stx) type 1 (Stx1) and/or type 2
46 (Stx2). A new toxin, belonging, like Stx to the AB₅ family, called Subtilase cytotoxin (SubAB)
47 was described in 2004 (2). It was initially isolated from the O113:H21 STEC strain 98NK2,
48 which was responsible for a HUS outbreak in Australia (2, 3). Very little is known of its role
49 in human pathology.

50 Although SubAB has been shown to bind with high specificity to glycans terminating in the
51 sialic acid N-glycolylneuraminic acid (Neu5Gc) (4) its specific receptors have not yet been
52 fully characterized. Studies show it can bind $\alpha 2\beta 1$ integrins, Hepatocyte growth factor
53 receptor (Met), NG2 and L1 cell adhesion molecule (LCAM1) (5). Once the B Subunit binds
54 to Neu5Gc, the toxin is internalized and travels via the retrograde pathway to the
55 endoplasmic reticulum (ER) where the catalytic A Subunit cleaves BiP (6). BiP is a major
56 chaperone and its cleavage leads to ER stress due to accumulation of unfolded proteins.
57 This represents a novel mechanism of action among bacterial cytotoxins. There are not
58 many *in vivo* studies describing SubAB action. When Wang et al. (7) inoculated mice
59 intraperitoneally (i.p.) with 5 μ g of SubAB, mice developed classical HUS lesions including
60 microangiopathic hemolytic anemia, thrombocytopenia and renal impairment.

61 Furthermore, the mice exhibited histopathological changes in kidney, brain, spleen and
62 liver with significant neutrophil infiltration in liver, spleen and kidney (7).

63 In another study, mice inoculated i.p. with 10 µg of purified SubAB developed severe
64 hemorrhage of the small intestine and died within 72 h. In the kidney they found
65 hyperplasia of the juxtaglomerular apparatus without renal failure. Organs including brain,
66 heart, lung, liver, spleen and pancreas subjected to routine histopathological analysis did
67 not show histopathological damage (8). The aim of this study was to characterize the
68 systemic effects caused in rats after i.p. inoculation of SubAB cytotoxin.

69

70 **2. MATERIAL AND METHODS**

71

72 **2.1 Animals**

73 Adult male Sprague-Dawley (SD) rats were obtained from the animal facility at the School
74 of Pharmacy and Biochemistry, University of Buenos Aires, Argentina. The rats were
75 individually housed under controlled conditions of illumination, humidity, and
76 temperature, with food and water being available ad libitum. Animals were allowed a
77 minimum of 7 days to adapt to housing conditions before undergoing any manipulation.

78 The experimental protocols and euthanasia procedures were reviewed and approved by
79 the Institutional Animal Care and Use Committee of the School of Medicine of University
80 of Buenos Aires, Argentina (CICUAL; Resolution No 2356/11). All the procedures were
81 performed in accordance with the EEC guidelines for care and use of experimental animals
82 (EEC Council 86/609).

83 **2.2 Experimental protocol**

84 Male SD rats (250 ± 1 g of body weight) were randomly divided into two groups of twelve
85 rats each. Group 1 (experimental group, $n = 12$) was i.p. inoculated with 10 μ L (1.5 μ g/ μ L)
86 of SubAB that corresponds to 60 ng SubAB/g of body weight (bwt). Group 2 (control
87 group, $n = 12$) was inoculated with the same volume of saline solution. Every experiment
88 was repeated three times. Half of the animals of each group ($n= 6$) were killed at 2 days
89 post inoculation. The rest of the animals were maintained for 20 days. At the moment of
90 sacrifice rats were anesthetized (100 μ g ketamine and 10 μ g diazepam/g bwt, i.p.) and
91 perfused with 4% paraformaldehyde.

92 SubAB cytotoxin was purified and characterized as previously described (7)

93

94 **2.3 Renal function**

95 To study renal function, rats were kept in metabolic cages for 24 h prior to sacrifice to
96 collect urine samples. Blood samples were obtained by cardiac puncture prior to sacrifice.
97 Plasma creatinine was assessed using a commercial kit (Wiener Lab, Rosario, Argentina).
98 Proteinuria (pyrogallol red-molybdate [colorimetric], Alcyon 300I analyzer, Abbott
99 Laboratories, Chicago, IL) and microalbuminuria (nephelometry IMMAGE, Beckman
100 Coulter, Brea, CA) were also measured.

101

102 **2.4 Histological and immunofluorescence studies**

103 Kidneys, liver and distal colon were fixed in 10% neutral formalin in PBS 0.1 M (pH: 7.4).

104 The tissue sections were dehydrated and embedded in paraffin. Sections of 5 μ m were

105 prepared with a microtome (Leica RM 2125, Wetzlar, Germany) and mounted on 2%
106 silane-coated slides. The sections were stained with Hematoxylin-Eosin (H-E), Periodic
107 Acid-Schiff stain (PAS), or Mallory's trichrome. The sections were then observed by light
108 microscopy (Nikon Eclipse 200, NY, USA).

109 For immunofluorescence studies, the slides were preincubated with non immune rabbit
110 serum in PBS (1:50) at room temperature for 30 min, followed by incubation with a
111 polyclonal anti-megalin (1:50, Santa Cruz Biotechnology, Santa Cruz, CA) antibody
112 overnight in a humidified chamber at 4°C. After several washes in PBS, the slides were
113 incubated with an anti-rabbit IgG antibody conjugated with fluorescein (1:200, Santa Cruz
114 Biotechnology) for 1 h at room temperature in a humidified chamber. Finally, all the slides
115 were mounted on a mixture containing PBS:glycerol (1:3), and observed in an
116 epifluorescent microscope (Nikon Eclipse E200, Nikon, Tokyo, Japan). Negative control
117 was performed without primary antibody.

118

119 **2.5 Electron Microscopy**

120 Renal cortical tissue was minced into 1 mm³ and tissues were fixed in 2 % glutaraldehyde
121 in 0.1 M sodium cacodylate buffer, pH 7.4, overnight at 4 °C, rinsed, post fixed in 1 %
122 osmium tetroxide in cacodylate buffer for 1 h at room temperature and rinsed. Then
123 sections were dehydrated through a graded series of ethanol and infiltrated with Epon
124 resin (Ted Pella) in a 1:1 solution of Epon and ethanol overnight. Sections were then
125 placed in fresh Epon for several hours and embedded in Epon overnight at 60 °C.

126 Ultrathin sections were cut on a Reichert ultramicrotome (Depew, NY) using a diamond
127 knife and transferred to Formvar/carbon-coated copper grids and contrasted in 2% uranyl
128 acetate and lead nitrate. Sections were then examined using Zeiss OM 109 transmission
129 electron microscope (Zeiss, Oberkochen, Germany).

130

131 **2.6 Molecular studies**

132 One kidney from experimental and control rats was excised prior to perfusion and
133 homogenized in HEPES buffer (0.01 M, pH 7.4) with protease inhibitors for Western
134 blotting SV Total RNA Isolation System (Promega, USA) buffer for RT-PCR analysis. They
135 were then frozen at -80°C until the time of the study.

136

137 **2.6.1 Western Blot**

138 The protein concentration in samples was determined with the BCA Protein Assay Kit
139 (Pierce Biotechnology Inc., Rockford, Ill., USA). Samples of 100 µg were electrophoresed
140 using 12.5% gels and electroblotted. Blots were incubated with rabbit polyclonal anti-TGF-
141 β1, or anti-FSP-1 antibodies (1: 1,000 ABCAM, USA) and horseradish peroxidase-
142 conjugated goat anti-rabbit IgG antibody (1: 3,000 Bio-Rad, Hercules, Calif., USA). To
143 determine the uniformity of loading, protein blots were probed with monoclonal anti- β-
144 actin antibody (1: 1,000 Sigma-Aldrich). Band intensities were measured using the
145 Quantity One densitometry software package (BioRad, USA). Protein bands were
146 normalized to their respective β-actin bands. The immunoblot analysis was carried out on
147 three different tissue preparations from three independent experiments.

148 **2.6.2 RT-PCR**

149 Total mRNA was isolated from kidney homogenate using an SV Total RNA Isolation system
150 (Promega Co.) and reverse transcription (RT) was performed for 60 min using Moloney
151 murine leukemia virus reverse transcriptase, oligo-dT15 primer and 400 μ M for each of
152 deoxyribonucleotide triphosphate (dNTP) at 42°C. Polymerase chain reaction (PCR) (35
153 cycles at 94°C for 60 s, 58°C for 60s and 72°C for 60 s followed by a final extension of 10
154 min at 72°C) was carried out using 5 μ M of designed specific oligonucleotide primers with
155 a sequence common to megalin (sense 5'-CATTGACGTGGTCAACTTGG-3' and antisense 5'-
156 CGAGTACCGTCTTCCTTTG-3'). These primers were designed using Broad Institute,
157 Primer3, available at: <http://wwwgenome.wi.mit.edu/science/software/software>, on the
158 basis of GenBank sequences. Negative control was performed without the addition of
159 reverse transcriptase, to confirm the absence of genomic DNA amplification. RT-PCR
160 products obtained were cloned and sequenced. Primers were used to β -actin as internal
161 standard. Densitometry of bands was carried out using the software ImajeJ1.44[®] (Wayne
162 Rasband, National Institutes of Health, USA).

163

164 **2.7 Statistical analysis**

165 All data are presented as mean \pm SEM; n = number of rats. Statistical analysis was
166 performed using the Graph Pad Prism Software 5.0 (San Diego, CA, USA). Differences
167 between experimental and control rats were analyzed by Student t-test. Statistical
168 significance was set at $P < 0.05$.

169

170 **3. RESULTS**

171

172 **3.1 Macroscopical findings**

173 Rats treated with a sublethal dose of SubAB (60 ng/g bwt) exhibited a marked increase of
174 abdominal cavity compatible with the development of ascites at 20 days post-inoculation
175 (Figure 1A). Puncture of the abdominal cavity showed the presence of a milky whitish
176 liquid which rapidly coagulated. This fluid was also detected when the thoracic cavity was
177 opened. Microscopic examination of the ascitic fluid revealed the presence of an
178 eosinophilic material with neutrophil infiltration (Figure 1B). The liver showed a
179 macronodular appearance with adherences (Figure 1C,D). In addition, the heart showed
180 concentric hypertrophy (88% of animals) or eccentric hypertrophy (12%) (Figure 1 E-G).
181 Biochemical analysis of the retrieved fluid detected cholesterol (51.5 ± 2.1 mg/dL),
182 triglycerides (82.5 ± 19.1 mg/dL), albumin (1.4 ± 0.1 g/l) and glucose (101 ± 25.5 mg/dL).

183

184 **Figure 1: Macroscopical findings in SubAB-treated rats.** Abdominal distention due to fluid
185 accumulation was evident 20 days post inoculation of SubAB. The abdominal puncture
186 showed the presence of a milky whitish liquid of very rapid coagulation (A). Eosinophilic
187 material with neutrophil infiltration was also detected (arrows, B). Abdominal organs
188 presented debris and adhesion (C) and liver had nodular appearance with adherences
189 (D).The heart showed eccentric hypertrophy (F) and concentric hypertrophy (G) compared
190 with the control (E).

191 **3.2 General and Renal parameters**

192 SubAB treated-rats showed a significant increase in microalbuminuria at 20 days post
 193 inoculation (Table 1). Other parameters such as water intake, urine output, plasma
 194 creatinine and proteinuria were not altered by the toxin treatment (Table 1).

195 **Table 1: General and renal parameters**

196

Parameter	Control group (n=18)		SubAB, 60 ng/g bwt (n= 18)	
	2 days	20 days	2 days	20 days
Microalbuminuria (mg/day)	0.06 ± 0.01	0.07 ± 0.01	0.07 ± 0.01	0.12 ± 0.01*
Proteinuria (mg/day)	4.1 ± 0.8	6.9 ± 1.6	3.8 ± 0.6	6.0 ± 2.2
Plasma creatinine (mg/dL)	0.75 ± 0.05	0.65 ± 0.02	0.67 ± 0.04	0.70 ± 0.03
Water intake (ml/day)	26.0 ± 3.6	39.8 ± 7.9	18.7 ± 3.2	30.7 ± 8.4
Urine output (ml/day)	23.0 ± 4.6	31.7 ± 10.1	15.79 ± 3.2	26.1 ± 6.7

197 * $p < 0.01$ experimental versus control group. SubAB-treated rats showed an increase in
 198 microalbuminuria 20 days post inoculation. Other parameters such as proteinuria, plasma
 199 creatinine, water intake and urine output were not altered by toxin treatment.

200

201 **3.3 Histopathological damage**

202 Histological analysis of colon and liver from rats treated with SubAB showed similar
 203 alterations at 2 and 20 days post inoculation (Table 2). On the kidney, significant

204 alterations were observed at 2 days and being more pronounced at 20 days (Table 2).
205 Figure 2 shows significant lesions in colon (B-D) and liver (F-H) from SubAB-treated rats
206 after 2 days of inoculation compared with the controls (A and E). In colon, detachment of
207 surface colonic cells (arrowhead in B), interstitial hemorrhagic foci (asterisks in C) and
208 Peyer's patches activation with mononuclear cell invasion of intestinal mucosa (arrow in
209 D) were detected. In liver, hepatocyte vacuolization (star in F), histoarchitecture distortion
210 (G) and neutrophil cell infiltration (arrow in H) were observed.

211 In kidney tissue, glomeruli and tubules exhibited a significant necrosis at 2 days post
212 inoculation of SubAB (Figure 3 B and D) compared with the controls (A and C). Glomeruli
213 showed necrosis, mesangial proliferation and capillary thickening at 20 days post
214 inoculation (Figure 3F). By Mallory's Trichrome staining, the number of glomeruli with
215 segmental fibrosis significantly increased after SubAB treatment (H). Quantification of
216 number of glomeruli with fibrosis (10 fields, 200×) is showed in Figure 3I (* $p < 0.001$). These
217 damages were not observed in control glomeruli (E and G).

218 To further examine the glomerular lesion, electron microscopy studies were performed.
219 Subepithelial nodules corresponding to actin filament condensation of the podocytes
220 were detected (TC in Figure 4B), indicating a disruption in normal podocyte cytoskeleton.
221 Foot process effacement (red arrow in C) and villous transformation (VT in B) were also
222 present. Normal filtration barrier was observed in glomeruli from control rats (Figure 4A).

223

224

225

226 **Table 2: Histological alterations in rat tissues after SubAB inoculation**

Tissue/Alteration	2 days post inocuation	20 days post inoculation
Colon		
Detachment of epithelial cells	Yes	Yes
Hemorrhagic foci	Yes	No
Peyer's patches activation	Yes	No
Mononuclear cell infiltration	No	Yes
Liver		
Hepatocyte vacuolization	Yes	Yes
Hystoarchitecture distortion	Yes	Yes
Neutrophil infiltration	Yes	Yes
Necrotic foci	No	Yes
Kidney		
Glomerular necrosis	Yes	Yes
Tubular necrosis	Yes	Yes
Mesangial proliferation	No	Yes
Capillary thickening	No	Yes
Focal and segmental fibrosis	No	Yes

227

228

229

230 **Figure 2: Ligth microscopy of colon and liver histological sections from SubAB-treated**
231 **rats.** Detachment of epithelial cells (arrowhead, B); hemorrhagic foci (asterisks, C) and
232 Peyer's patches activation with mononuclear cell invasion of intestinal mucosa (arrow, D)
233 were observed in the colon from SubAB-treated rats compared to the Control rats (A).
234 Vacuolization of hepatocytes (black star, F); histoarchitecture distortion (G) and neutrophil
235 infiltration (arrow, H) was observed. Normal histoarchitecture was observed in liver from
236 control rats (E). Staining with hematoxilin-eosin (A-H).

237

238

239 **Figure 3: Ligth microscopy of kidney histological sections from SubAB-treated rats.**
240 Necrosis in glomeruli (arrowhead, B) and renal tubules (arrowhead D) was detected at 2
241 days post inoculation of SubAB (60 ng/Kg). At 20 days post inoculation, glomeruli showed
242 necrosis, mesangial proliferation, capillary thickening (black arrows in F) and segmental
243 fibrosis (black asterisk in H). Quantification of number of glomeruli with fibrosis (10 fields,
244 200×) is showed in I (*p<0.001). Kidney sections from control rats (A, C, E, G). Staining with
245 PAS (A-F) and with Mallory's Trichrome (G-H) were performed.

246

247 **Figure 4: Electromicroscopy of glomeruli from SubAB-treated rats at 20 days post**
248 **inoculation.** Ultrastructural study revealed foot process effacement (red arrow in C),
249 villous transformation (VT in B) and actin tono filament condensation (TC in B). Control (A).

250 **Molecular studies**

251

252 **3.4 TGF- β and FSP1 protein expression**

253 Expression of TGF- β protein (12.5 kDa) was examined in kidney tissues from Control and
254 SubAB-treated rats at 20 days post inoculation by WB (Figure 5A). The mean TGF- β levels
255 normalized to β -actin showed a significant increase after SubAB treatment (Figure 5B).

256 Taking into account that TGF- β triggers EMT (9) and that FSP1 is a marker of fibroblasts
257 present in EMT, the expression of FSP1 (12 kDa) was examined by WB (Figure 5C). The
258 mean FSP1 levels normalized to β -actin were also significantly increased in rats treated
259 with SubAB (Figure 5D).

260

261 **3.5 Expression of megalin protein and mRNA**

262 Figure 6 shows a representative immunofluorescence staining for megalin in renal
263 proximal tubules from rats sacrificed at 20 days post inoculation of SubAB. Reduced label
264 in SubAB-treated rats (B) was observed compared with the controls (A). In order to
265 determine if the reduction in protein levels may be correlated with a decrease in megalin
266 mRNA, RT-PCR analysis were performed. Figure 6C shows an expected band
267 corresponding to megalin expression in kidney from control but not from SubAB-treated
268 rats. The average megalin mRNA levels normalized to β -actin indicate that the decrease in
269 megalin protein is due to a decrease in mRNA expression (Figure 6D).

270

271 **Figure 5: TGF- β and FSP1 expression in renal tissue from SubAB treated-rats at 20 days**
272 **post inoculation.** TGF- β (A) and FSP1 (C) proteins were detected in kidney homogenates

273 by Western blot. Bar graphs represents the average protein levels normalized to the
274 loading control β -actin (B, D). n= 6 ,*p<0.001.

275

276 **Figure 6: Megalin expression in kidney from SubAB-treated rats at 20 days post**
277 **inoculation.** Renal tissue showed a decrease in megalin expression (B) compared to
278 controls (A) by indirect immunofluorescence and by RT-PCR (C). Bar graphs represents the
279 average megalin levels normalized to β -actin (D, n = 6, *p< 0.001)

280

281 4. DISCUSSION

282 The main findings after intraperitoneal SubAB inoculation in rats were the development of
283 ascites, cardiac hypertrophy and histological alterations in colon, liver and kidney. These
284 findings are consistent with a systemic inflammatory response to the toxin described by
285 Furukawa et al. after intraperitoneal inoculation of 10 μ g of SubAB in mice (8). After 2 days
286 of treatment with SubAB, we found hemorrhagic foci with mucosal erosion in the rat colon
287 without macroscopic alterations of the small bowel. The animals did not develop diarrhea
288 as previously described (7). Nevertheless, previous studies showed SubAB is able to inhibit
289 the net water absorption across human colonic mucosa (10). Taking into account there
290 have been reports of diarrhea in patients infected with bacterial strains which produce
291 SubAB but not Stx2 (11), more studies are necessary to clarify the differences observed
292 between the clinical setting and the observations made in animal studies.

293 In addition, we have detected neutrophil infiltration in several tissues in agreement with
294 results described by Wang et al. (7). We have also observed cytoplasmic vacuoles in the
295 hepatocytes. Vacuole formation has been previously reported in *in vitro* studies (12, 13).
296 Lass et al. (12, 13) described vacuole formation in HeLa cells after a period of 6 h of
297 incubation with SubAB (1 μ g/ml). Currently the cause underlying vacuole formation due to
298 SubAB inoculation remains unknown although it may be linked to SubAB receptors. Little
299 information is available regarding the precise identity and distribution of SubAB receptors
300 (7). Further studies characterizing them could throw some light on why vacuoles were not
301 found in other tissues.

302 Regarding the ascites, its development has not been previously described after the
303 inoculation of either SubAB or Stx2. HUS patients have never been reported to develop
304 peritoneal effusion neither has it been described in any HUS animal model. Taking into
305 account the biochemical and histological analysis performed on the ascitic fluid, we
306 suggest it could be related with an inflammatory response induced by the SubAB
307 cytotoxin.

308 Our study is the first to describe SubAB action on the heart. We found the development of
309 concentric cardiac hypertrophy in 88% of the animals and eccentric cardiac hypertrophy in
310 12%. Physiopathological mechanisms that govern the development of the hypertrophy are
311 different, being either pressure or volume overload. HUS patients have been known to
312 develop cardiac hypertrophy, but there aren't enough studies on extra-renal HUS
313 manifestations (14). As SubAB is only now emerging as a pathogenic factor, its
314 contribution to this finding cannot be ruled out.

315 Although plasma levels of creatinine, which is a marker of kidney injury were not altered
316 in rats neither at 2 nor at 20 days they presented histopathological damage. In agreement
317 with our results studies performed by Vaidya et al. show that serum creatinine was a poor
318 predictor of renal injury in various structurally and mechanistically different models of
319 renal tubular injury in rats (15). There is also evidence that serum creatinine has poor
320 sensitivity when there is adequate renal reserve. In this case its levels may not be changed
321 due to compensatory increases in the function of other nephrons (16).

322 Whereas plasma creatinine is a conventional marker to monitor kidney injury in humans,
323 histopathology constitutes the gold standard for animal models (15). ~~We also found~~

324 Although plasma creatinine levels were not altered, we did find development of
325 microalbuminuria 20 days post inoculation of SubAB. This led us to further study the renal
326 protein handling mechanisms. Development of microalbuminuria could be produced by an
327 alteration in glomerular filtration and/or tubular protein reabsorption. SubAB caused
328 podocyte villous transformation, foot process effacement and actin filament condensation
329 and decreased megalin expression in proximal tubules. One of the ways in which proteins
330 can be reabsorbed in tubules is megalin dependent (17). These facts could explain the
331 presence of albumin in urine.

332 Yahiro et al. (5) identified $\alpha 2\beta 1$ integrin as SubAB receptor. Podocytes bind to the basal
333 membrane by a $\alpha 2\beta 1$ integrin (18, 19). Concerning SubAB effects on the podocytes, we
334 suggest that SubAB could directly affect the podocytes interacting with the $\alpha 2\beta 1$ integrin.

335 Podocyte villous transformation, actin filament condensation and glomerular necrosis with
336 adherences may develop following mesangiolytic. Mesangial proliferation has been

337 associated with podocyte dysfunction and local TGF- β production, both of which are
338 present in SubAB-treated rats. We found TGF- β is increased 20 days post inoculation. TGF-
339 β would act by promoting fibroblast and mesangial cell growth and extracellular matrix
340 accumulation (20). Taking into account that TGF- β triggers EMT (1) and that FSP1 is a
341 marker of fibroblasts present in EMT, our results suggest that SubAB may progress
342 towards tubule interstitial fibrosis (21).

343 SubAB cytotoxin produced a decrease in kidney megalin levels. This alteration could be
344 due to the increase in TGF- β involved in megalin recycling to the apical membrane of renal
345 proximal tubule cells. In previous studies, we reported that an increase of TGF- β
346 expression which caused a decrease in megalin levels was responsible of
347 microalbuminuria in Stx2-treated rats (22). The ability of SubAB to alter megalin
348 expression in renal proximal tubules from SubAB-treated rats would in part explain the
349 development of microalbuminuria.

350 Taking all this into account it is important to consider the effects produced by the toxin
351 both at 2 and 20 days. At 2 days the toxin produced a multiorganic lesion, that although it
352 was histologically observed, it did not lead to the death of the animals. At 20 days
353 postinoculation we could still find organ damage as that seen at 2 days with new
354 developments including cardiac hypertrophy, ascites and glomerular fibrosis in the kidney.
355 This shows that acute damage produced by the toxin is not self-limiting and evolves to
356 chronicity into a complex clinical picture, which could probably lead to animal death.
357 Further studies are needed to address the mechanisms underlying the observed organ
358 damage, and how the clinical picture evolves.

359 In conclusion we have described the action of SubAB cytotoxin on the heart developing
360 cardiac hypertrophy, and on the liver where it elicits vacuole formation. In particular, in
361 the kidney, SubAB is able to damage podocytes, trigger EMT and alter the renal protein
362 handling by disruption of the filtration barrier and tubular protein reabsorption.

363

364 **FUNDING INFORMATION**

365 This research received specific grant from Buenos Aires University UBACyT
366 20020130200223BA and PICT-0777-ANPCYT

367

368 **ACKNOWLEDGEMENTS**

369 The authors thank to Pablo Cepero for excellent technical assistance

370

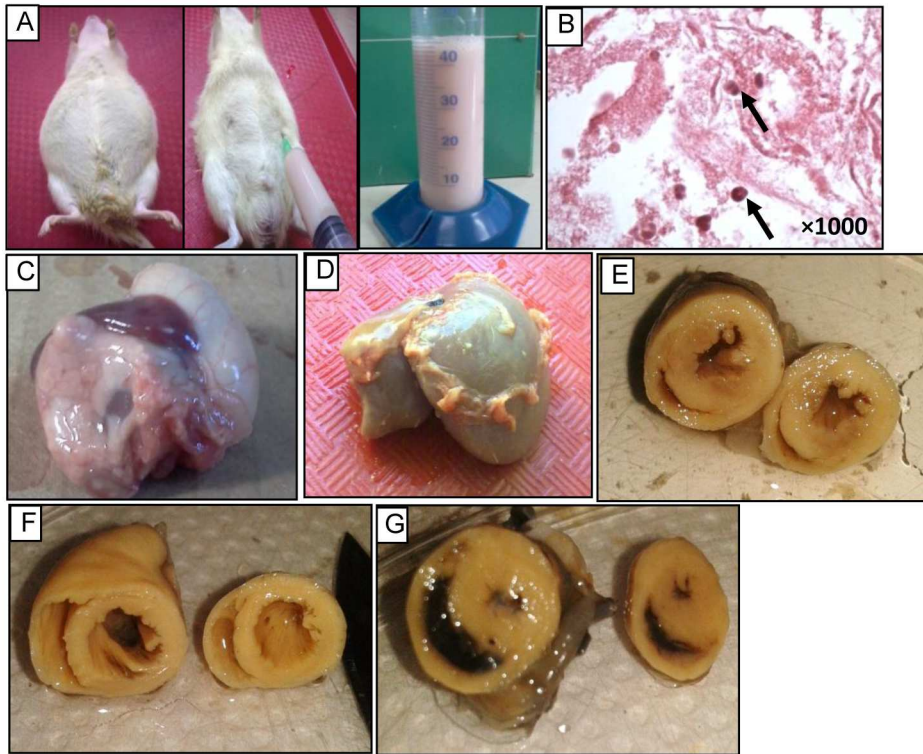
371 **REFERENCES**

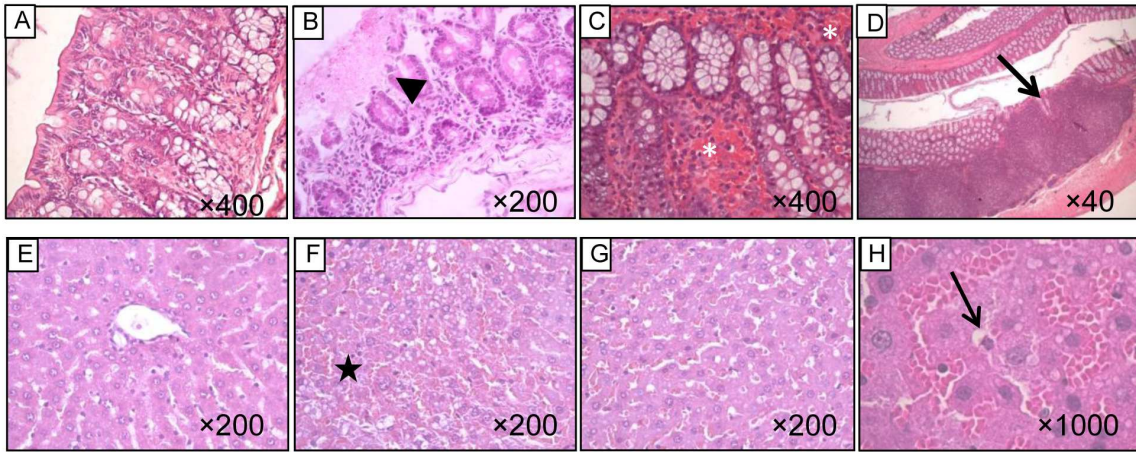
- 372 1. **Wuyts W, Van Hul W, Wauters J, Nemtsova M, Reyniers E, Van Hul EV, De Boule K, de**
373 **Vries BB, Hendrickx J, Herrygers I, Bossuyt P, Baemans W, Fransen E, Vits L, Coucke P,**
374 **Nowak NJ, Shows TB, Mallet L, van den Ouweland AM, McGaughan J, Halley DJ, Willems**
375 **PJ.** 1996. Positional cloning of a gene involved in hereditary multiple exostoses. *Hum Mol*
376 *Genet* **5**:1547-1557.
- 377 2. **Paton AW, Srimanote P, Talbot UM, Wang H, Paton JC.** 2004. A new family of potent
378 AB(5) cytotoxins produced by Shiga toxigenic *Escherichia coli*. *J Exp Med* **200**:35-46.
- 379 3. **Paton AW, Paton JC.** 2005. Multiplex PCR for direct detection of Shiga toxigenic
380 *Escherichia coli* strains producing the novel subtilase cytotoxin. *J Clin Microbiol* **43**:2944-
381 2947.
- 382 4. **Byres E, Paton AW, Paton JC, Lofling JC, Smith DF, Wilce MC, Talbot UM, Chong DC, Yu H,**
383 **Huang S, Chen X, Varki NM, Varki A, Rossjohn J, Beddoe T.** 2008. Incorporation of a non-
384 human glycan mediates human susceptibility to a bacterial toxin. *Nature* **456**:648-652.
- 385 5. **Yahiro K, Morinaga N, Satoh M, Matsuura G, Tomonaga T, Nomura F, Moss J, Noda M.**
386 2006. Identification and characterization of receptors for vacuolating activity of subtilase
387 cytotoxin. *Mol Microbiol* **62**:480-490.
- 388 6. **Paton AW, Beddoe T, Thorpe CM, Whisstock JC, Wilce MC, Rossjohn J, Talbot UM, Paton**
389 **JC.** 2006. AB5 subtilase cytotoxin inactivates the endoplasmic reticulum chaperone BiP.
390 *Nature* **443**:548-552.
- 391 7. **Wang H, Paton JC, Paton AW.** 2007. Pathologic changes in mice induced by subtilase
392 cytotoxin, a potent new *Escherichia coli* AB5 toxin that targets the endoplasmic reticulum.
393 *J Infect Dis* **196**:1093-1101.
- 394 8. **Furukawa T, Yahiro K, Tsuji AB, Terasaki Y, Morinaga N, Miyazaki M, Fukuda Y, Saga T,**
395 **Moss J, Noda M.** 2011. Fatal hemorrhage induced by subtilase cytotoxin from Shiga-
396 toxigenic *Escherichia coli*. *Microb Pathog* **50**:159-167.
- 397 9. **Meng XM, Nikolic-Paterson DJ, Lan HY.** 2016. TGF-beta: the master regulator of fibrosis.
398 *Nat Rev Nephrol*.
- 399 10. **Gerhardt E, Masso M, Paton AW, Paton JC, Zotta E, Ibarra C.** 2013. Inhibition of water
400 absorption and selective damage to human colonic mucosa are induced by subtilase
401 cytotoxin produced by *Escherichia coli* O113:H21. *Infect Immun* **81**:2931-2937.
- 402 11. **Tozzoli R, Caprioli A, Cappannella S, Michelacci V, Marziano ML, Morabito S.** 2010.
403 Production of the subtilase AB5 cytotoxin by Shiga toxin-negative *Escherichia coli*. *J Clin*
404 *Microbiol* **48**:178-183.
- 405 12. **Lass A, Kujawa M, McConnell E, Paton AW, Paton JC, Wojcik C.** 2008. Decreased ER-
406 associated degradation of alpha-TCR induced by Grp78 depletion with the SubAB
407 cytotoxin. *Int J Biochem Cell Biol* **40**:2865-2879.
- 408 13. **Morinaga N, Yahiro K, Matsuura G, Watanabe M, Nomura F, Moss J, Noda M.** 2007. Two
409 distinct cytotoxic activities of subtilase cytotoxin produced by shiga-toxigenic *Escherichia*
410 *coli*. *Infect Immun* **75**:488-496.
- 411 14. **Gallo EG, Gianantonio CA.** 1995. Extrarenal involvement in diarrhoea-associated
412 haemolytic-uraemic syndrome. *Pediatr Nephrol* **9**:117-119.
- 413 15. **Vaidya VS, Ozer JS, Dieterle F, Collings FB, Ramirez V, Troth S, Muniappa N, Thudium D,**
414 **Gerhold D, Holder DJ, Bobadilla NA, Marrer E, Perentes E, Cordier A, Vonderscher J,**
415 **Maurer G, Goering PL, Sistare FD, Bonventre JV.** 2010. Kidney injury molecule-1
416 outperforms traditional biomarkers of kidney injury in preclinical biomarker qualification
417 studies. *Nat Biotechnol* **28**:478-485.
- 418 16. **Waikar SS, Betensky RA, Emerson SC, Bonventre JV.** 2012. Imperfect gold standards for
419 kidney injury biomarker evaluation. *J Am Soc Nephrol* **23**:13-21.

- 420 17. **Dickson LE, Wagner MC, Sandoval RM, Molitoris BA.** 2014. The proximal tubule and
421 albuminuria: really! *J Am Soc Nephrol* **25**:443-453.
- 422 18. **Saleem MA.** 2015. One hundred ways to kill a podocyte. *Nephrol Dial Transplant* **30**:1266-
423 1271.
- 424 19. **Sachs N, Sonnenberg A.** 2013. Cell-matrix adhesion of podocytes in physiology and
425 disease. *Nat Rev Nephrol* **9**:200-210.
- 426 20. **Loeffler I, Wolf G.** 2014. Transforming growth factor-beta and the progression of renal
427 disease. *Nephrol Dial Transplant* **29 Suppl 1**:i37-i45.
- 428 21. **Lovisa S, LeBleu VS, Tampe B, Sugimoto H, Vадnagara K, Carstens JL, Wu CC, Hagos Y,
429 Burckhardt BC, Pentcheva-Hoang T, Nischal H, Allison JP, Zeisberg M, Kalluri R.** 2015.
430 Epithelial-to-mesenchymal transition induces cell cycle arrest and parenchymal damage in
431 renal fibrosis. *Nat Med* **21**:998-1009.
- 432 22. **Ochoa F, Oltra G, Gerhardt E, Hermes R, Cohen L, Damiano AE, Ibarra C, Lago NR, Zotta E.**
433 2012. Microalbuminuria and early renal response to lethal dose Shiga toxin type 2 in rats.
434 *Int J Nephrol Renovasc Dis* **5**:29-36.

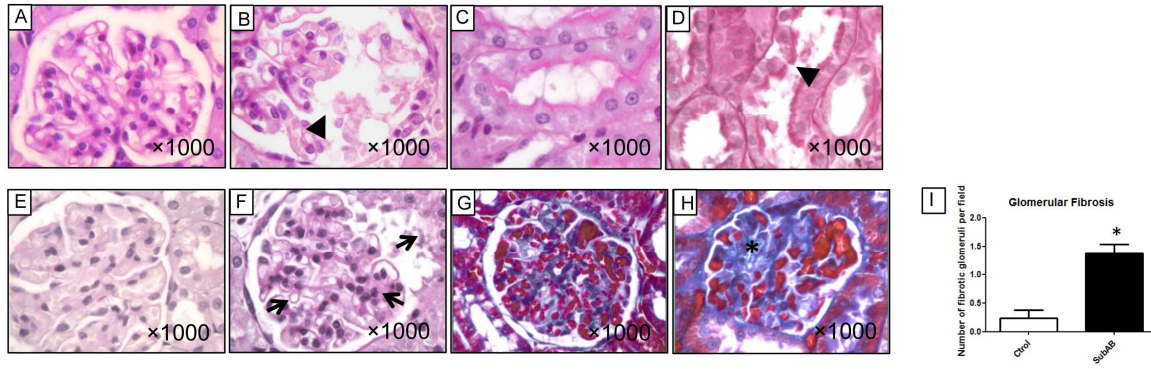
435

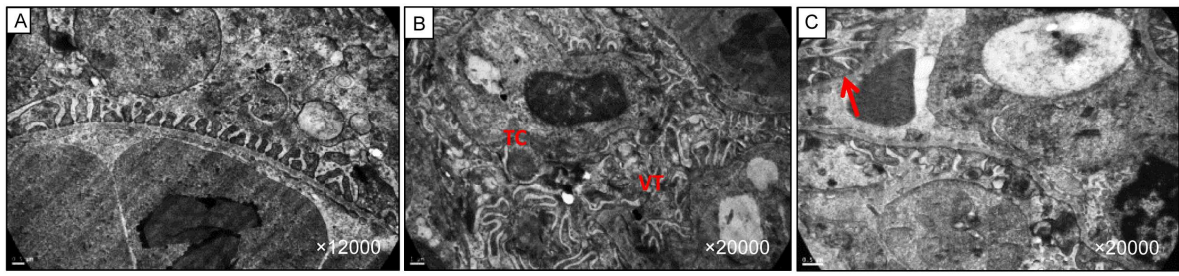
436



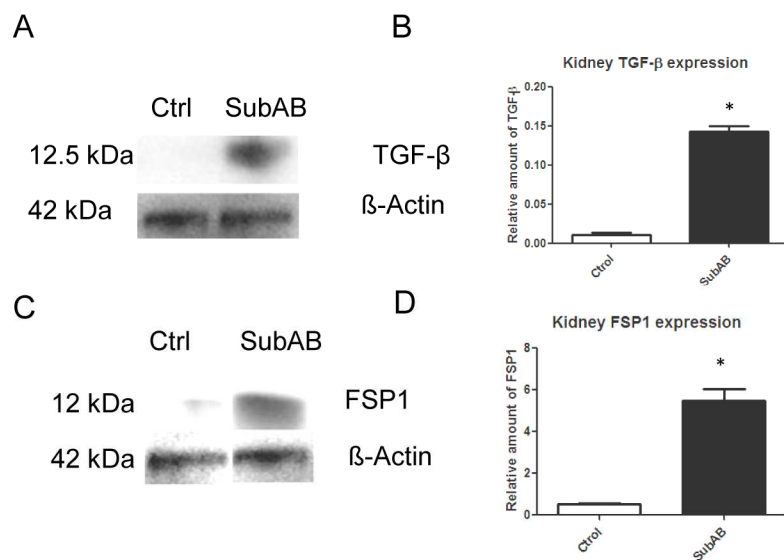


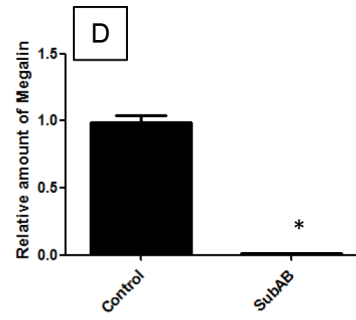
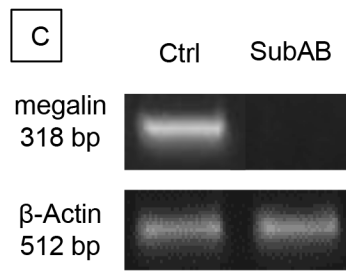
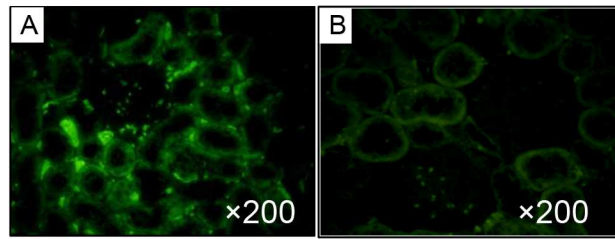
ACCEPTED MANUSCRIPT





ACCEPTED MANUSCRIPT





Highlights:

- We report novel effects of SubAB cytotoxin *in vivo*
- Rats develop ascites 20 days after SubAB inoculation
- SubAB is capable of triggering cardiac hypertrophy
- SubAB elicits vacuole formation in the liver
- SubAB alters podocytes cytoskeleton and tubular renal protein handling

Ethical Statement for Toxicon

I testify on behalf of all co-authors that our article submitted to Toxicon

Title: **Systemic effects of Subtilase cytotoxin produced by *Escherichia coli* O113:H21**

All authors: **Abril Seyahian, Gisela Oltra, Federico Ochoa, Santiago Melendi, Ricardo Hermes, James C. Paton, Adrienne W. Paton, Nestor Lago, Mauricio Castro Parodi, Alicia Damiano, Cristina Ibarra, Elsa Zotta**

- 1) this material has not been published in whole or in part elsewhere;
- 2) the manuscript is not currently being considered for publication in another journal;
- 3) all authors have been personally and actively involved in substantive work leading to the manuscript, and will hold themselves jointly and individually responsible for its content.

Date:20/10/2016

Corresponding author's signature: Elsa Zotta